

# Thermal Dynamics in Symmetric Magnetic Nanopillars Driven by Spin Transfer

Weng L. Lim, Nicholas Anthony, Andrew Higgins, and Sergei Urazhdin  
*Department of Physics, West Virginia University, WV 26506*

We study the effects of spin transfer on thermally activated dynamics of magnetic nanopillars with identical thicknesses of the magnetic layers. The symmetric nanopillars exhibit anomalous dependencies of switching statistics on magnetic field and current. We interpret our data in terms of simultaneous current-induced excitation of both layers. We also find evidence for coupling between the fluctuations of the layers due to the spin transfer.

PACS numbers: 72.25.Ba, 75.50.Ee, 75.60.Jk, 75.70.Cn

Spin polarized current flowing through a nanoscale magnet  $F_1$  can change its magnetic configuration due to the spin transfer torque (ST) [1, 2]. Real devices require an additional nanomagnet  $F_2$  to polarize the current flowing through  $F_1$ . To minimize the complications due to the ST exerted on the polarizing layer  $F_2$ , it is usually made much thicker than  $F_1$ , or pinned by an adjacent antiferromagnet via exchange bias. In this case, the magnitude of the current required to induce dynamics in  $F_2$  is expected to be much larger than in  $F_1$ . However, simultaneous effects of ST on several magnetic layers are important in many devices such as those incorporating artificial antiferromagnets, which are comprised of two or more magnetic layers of similar thickness. Understanding these effects is important for enhancing the performance and stability of magnetoelectronic devices.

In a symmetric bilayer comprised of two separate magnetic layers  $F_1$  and  $F_2$  with similar dimensions, the direction of ST exerted on both layers is the same. Consequently, ST has been suggested to induce their coupled precession in a propeller-like fashion [1]. Measurements of magnetoresistance (MR) in symmetric Co-based nanopillars showed resistance increases at large magnetic field  $H$  for both directions of the applied current  $I$  [5, 6]. These features were attributed to current-induced precession of  $F_1$  for one direction of current, and of  $F_2$  for the opposite direction. However, the relation of these results to the theoretical picture of ST is not clear.

In this Letter, we present measurements of the effect of ST on symmetric nanopillars in thermally activated regime, i.e. when the magnetic moments flip their directions randomly due to thermal fluctuations enhanced by ST. We show that the dynamics of both layers must be activated due to the simultaneous effect of ST on both layers. We develop a simple activation model, and present data indicating coupling between the dynamics of the two layers mediated by ST.

Our samples with structure  $F_1 = \text{Ni}_{80}\text{Fe}_{20} = \text{Py}(4)/\text{Cu}(3)/F_2 = \text{Py}(4)$  were deposited at room temperature (RT) by magnetron sputtering at base pressure of  $5 \times 10^{-9}$  Torr, in 5 mTorr of purified Ar. All thicknesses are in nm. The structure was patterned into a nanopillar with dimensions  $120 \times 60$  nm sandwiched between Cu leads by a process described elsewhere [7]. The patterning procedure resulted in slightly smaller

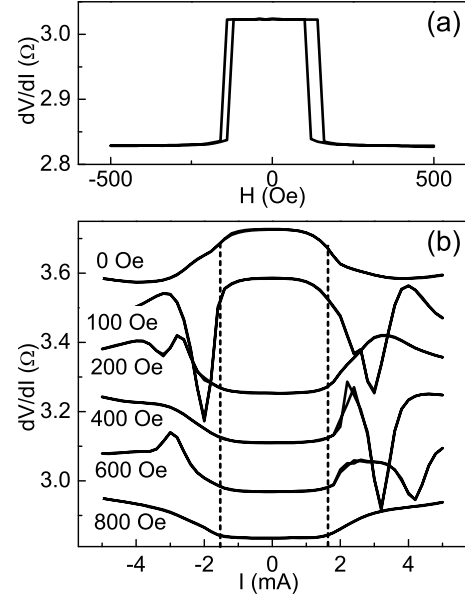


FIG. 1: (a)  $dV/dI$  vs.  $H$  at  $I = 0$ . (b)  $dV/dI$  vs.  $I$  at  $H = 0$  as labeled. The curves are offset for clarity.

dimensions of  $F_2$  than  $F_1$ , as shown by measurements of MR. This slight asymmetry is important for some of the behaviors described below. We measured  $dV/dI$  at RT with four-probes and lock-in detection, adding an ac current of amplitude not exceeding  $100 \mu\text{A}$  at 1 kHz to the dc current  $I$ . Positive  $I$  flows from  $F_1$  to  $F_2$ .  $H$  is in the film plane and along the nanopillar easy axis. We report results for one of the four samples tested with similar results.

In scans of field  $H$  at  $I = 0$ , the sample exhibits a nearly reversible transition from antiparallel (AP) state with resistance  $R_{AP}$  at small  $H$ , to parallel (P) state with resistance  $R_P$ , at field  $H_d \approx 137$  Oe characterizing the dipolar coupling between the magnetic layers (Fig. 1(a)). ST in asymmetric nanopillars has been characterized by a distinct asymmetric dependence of  $dV/dI$  on  $I$  [3]. In contrast, our samples show an approximately symmetric dependence of  $dV/dI$  on  $I$  (Fig. 1(b)). At  $H = 0$ , increasing the magnitude of  $I$  results in a gradual decrease of  $dV/dI$  starting from  $|I| \approx I_c = 1.6$  mA, as marked with dashed vertical lines.  $dV/dI$  reaches a minimum of

2.87  $\Omega$  at  $I = \pm 4$  mA, followed by a small increase at larger  $I$ . The minimum of  $dV/dI$  is larger than the P-state resistance  $R_P = 2.83 \Omega$ , indicating that a stable P state is not reached at any  $I$ . For  $H > 0$ , large variations of  $dV/dI$  appear at  $|I| > I_c$ , stabilizing at  $H > 600$  Oe into gradual increases. The data for  $H \geq 800$  Oe only weakly depend on  $H$ . We note a well-defined transition from the AP state at  $|I| < I_c$  and  $H \leq 100$  Oe, to a P state at  $H > 100$  Oe, consistent with the MR data of Fig. 1(a). We attribute the more systematic behaviors of our data compared to the results for Co-based nanopillars [5, 6] to the smaller dimensions of our nanopillars, indicated by a larger MR, and weaker random crystalline anisotropy of Py. These factors decrease the possibilities of inhomogeneous and noncollinear magnetic states.

Two distinct types of magnetic dynamics induced by ST have been established for asymmetric nanopillars [7, 8]. At  $H$  that was not too large, thermally activated flipping of the magnetic moment resulted in sharp peaks and/or cusps in differential resistance. ST-induced magnetic precession is induced at large  $H$ . It is usually characterized by smooth, nearly independent of  $H$  increases of MR. One may be tempted to attribute the large- $H$  behaviors of our symmetric samples to such precession. However, our microwave spectroscopic measurements, as well simulations using the Landau-Lifshits-Gilbert equations, show that coherent precession is destroyed due to the ST-induced coupling of the dynamics of two layers [4]. Instead, we focus here on the sharp features observed in our samples at  $|I| > I_c$  for  $H < 600$  Oe (Fig. 1(b)). Time-resolved measurements of resistance showed that these features are caused by thermally activated flipping of magnetic layers. The characteristics of the resulting telegraph noise (TN) discussed below dramatically differ from the usual properties of asymmetric samples [9], enabling us to unambiguously attribute them to the simultaneous effects of ST on both magnetic layers.

In the TN regime for asymmetric nanopillars at  $I > 0$ , the average dwell time  $\tau_P$  in the P state decreased with increasing  $I$ , while the dwell time  $\tau_{AP}$  in the AP state increased [9]. Increasing  $H$  had the opposite effect on  $\tau_P$  and  $\tau_{AP}$ . The results for symmetric nanopillars are shown in Fig. 2. We note that the MR in the TN measurements are consistent with the static data of Fig. 1(a), indicating single domain behaviors. At a fixed  $H = 120$  Oe, both  $\tau_P$  and  $\tau_{AP}$  decrease with increasing  $I > 0$ , remaining nearly equal over five orders of magnitude of their variation (Fig. 2(a)). These behaviors are not observed in asymmetric nanopillars, and therefore must be attributed to the effects of ST on both magnetic layers. Fig. 2(a) also shows that a different TN regime appears at a larger  $H = 260$  Oe. In this regime,  $\tau_{AP}$  increases with increasing  $I$ , while  $\tau_P$  decreases. These latter behaviors can be easily explained when the slight asymmetry of the nanopillar is taken into account. Large enough  $H$  must suppress the effects of ST on the larger  $F_1$ , resulting in behaviors similar to those seen before in nanopillars with a thick  $F_1$ .

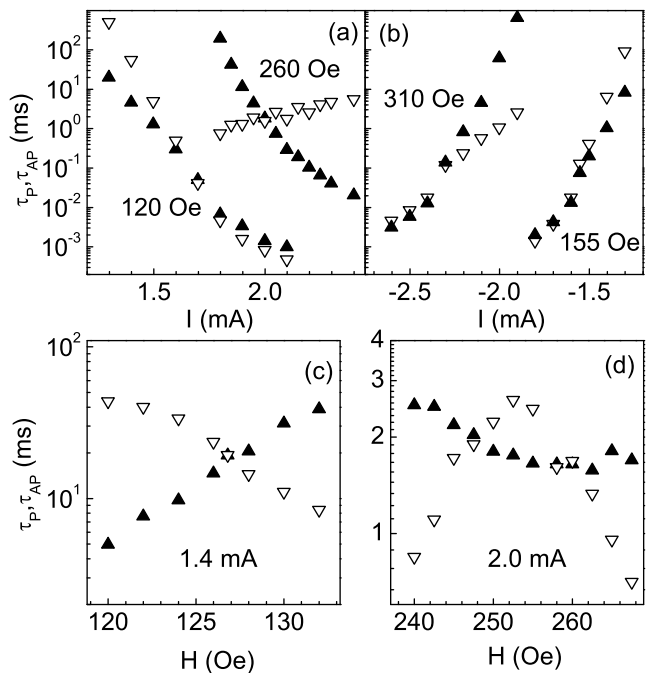


FIG. 2:  $\tau_P$  (solid symbols) and  $\tau_{AP}$  (open symbols) vs  $I$  at fixed  $H$  as labeled (a,b), and vs  $H$  at fixed  $I$  as labeled (c,d). The uncertainties are similar to the symbol sizes.

Because of the symmetry of the sample, one can expect to see TN at  $I < 0$  similar to that in Fig. 2(a) for  $I > 0$ . Indeed, Fig. 2(b) shows that the regime  $\tau_P = \tau_{AP}$  is also observed at  $I < 0$ , although at a somewhat different  $H = 155$  Oe. In the second regime at a larger  $H = 310$  Oe, both  $\tau_P$  and  $\tau_{AP}$  still decrease, but at different rates following the trend in Fig. 2(a). Dependencies on  $H$  shown in Figs. 2(c,d) explain the existence of two different TN regimes. At small  $H$  and  $I > 0$  (Fig. 2(c)),  $\tau_P$  increases, and  $\tau_{AP}$  decreases with increasing  $H$ . These trends become reversed twice at larger  $H$  (Fig. 2(d)). As a result, the condition  $\tau_P \approx \tau_{AP}$  is satisfied at least twice when  $H$  is increased. The complex nonmonotonic variations of dwell times in Fig. 2 explain the large irregular changes of MR in Fig. 1(a): small (on the logarithmic scale) relative changes of  $\tau_P$  with respect to  $\tau_{AP}$  result in variations of  $R$  between values very close to  $R_P$  and  $R_{AP}$ . These significant current-dependent variations of  $R$  appear as even sharper features in the differential resistance  $dV/dI$ .

We interpret our results with a model for the dwell time of a ferromagnet in the presence of ST [10]

$$\tau = \tau_0 \exp \left[ \frac{E(H)(1 - I/I_c)}{k_B T} \right], \quad (1)$$

where  $\tau$  is the dwell time in P or AP state,  $\tau_0$  is attempt time,  $E(H)$  is the activation barrier at  $I = 0$ ,  $I_c$  is the critical current for the onset of current-induced dynamics at  $T = 0$ , and  $k_B$  is the Boltzmann constant. For the following discussion, we combine  $k_B T / (1 - I/I_c)$  into

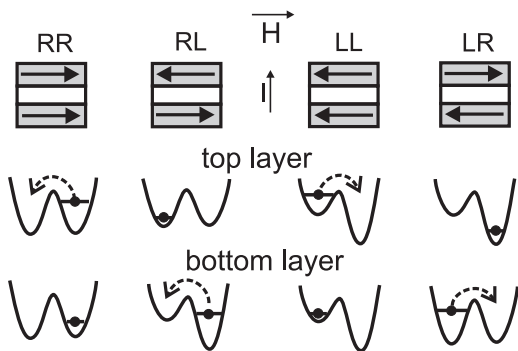


FIG. 3: Four magnetic configurations of symmetric nanopillars. Lower panels are schematics for the activation barriers and effective temperatures of the magnetic layers at  $I > 0$ . Dashed arrows show the transitions driven by ST, assuming that effects of ST on the fluctuations of the two layers are independent.

an effective current-dependent temperature  $T^*(I)$ , which has a physically transparent interpretation as describing the enhanced/suppressed by ST thermal fluctuations of the magnetic moment. Alternatively, one can describe the effect of ST in terms of a current-dependent effective barrier  $E(H, I)$  [11]. These two formally different approaches equally well describe the nearly uniform dynamics of the nanoscale magnetic layers.

Assume that the effects of ST on the fluctuations of  $F_1$  and  $F_2$  are independent. In this case, Eq. 1 can be used to separately determine the dwell times of each magnetic layer for every possible configuration of the nanopillar. In the P state, the critical current  $I_{C1}$  describing the ST-driven excitation of  $F_1$  is positive, while the critical current  $I_{C2}$  describing the ST-driven excitation of  $F_2$  is negative. In the AP state,  $I_{C1} < 0$  and  $I_{C2} > 0$ . According to Eq. 1, the effect of ST at  $I > 0$  is to increase the effective temperature  $T^*_{AP1}$  of  $F_1$  in the AP state, thus decreasing the corresponding dwell time  $\tau_{AP1}$ . Simultaneously, the effective temperature  $T^*_{AP2}$  of  $F_2$  is decreased, increasing its dwell time  $\tau_{AP2}$ . As a result,  $F_1$  flips with higher probability than  $F_2$ , bringing the system into the P state. The effective temperature  $T^*_{P2}$  of  $F_2$  in the P state is enhanced, resulting in its subsequent flipping into AP state. The cycle of sequential flipping of  $F_1$  and  $F_2$  is then repeated. By symmetry, a similar cycle

in reverse direction is expected for  $I < 0$ . This simplified model explains the simultaneous decreases of  $\tau_P$  and  $\tau_{AP}$  with  $I$  (Figs. 2(a,b)). However, analysis given below shows that it cannot fully account for the dependence of data on  $H$ , indicating that the assumption of independent effects of ST on  $F_1$  and  $F_2$  used in this model is not fully justified.

Taking into account external and dipolar fields requires one to consider four magnetic configurations denoted RR, RL, LL, and LR based on the directions (Left or Right) of  $F_1$  and  $F_2$ , as illustrated in Fig. 3 for  $I > 0$  and  $H \approx H_d$  pointing to the right. Describing the dwell times of both layers in each configuration by Eq. 1 yields a sequence of transitions RR-RL-LL-LR-RR, as shown by dashed arrows in the schematics of activation energies. Based on this analysis, one expects  $\tau_{LL} \ll \tau_{RR} \approx \tau_{LR} \ll \tau_{RL}$  for the dwell times in the corresponding configurations. This implies  $\tau_{AP} > \tau_P$ , which is inconsistent with the regime  $\tau_P = \tau_{AP}$  in Fig. 2. Moreover, increasing  $H$  should increase both  $\tau_{AP}$  which is dominated by the slow transition RL-LL, and  $\tau_P$  which is dominated by the slow transition RR-RL. This explains the  $H < 254$  Oe part of panel (d), but is inconsistent with the data of Fig. 2(c). These shortcomings of the model likely originate from the oversimplified assumption that the effects of ST on the fluctuations of two layers are independent. Indeed, considering the state RL, enhanced fluctuations of  $F_1$  due to ST must also induce fluctuations of  $F_2$  because ST exerted on both layers is similar in magnitude, coupling their dynamics [1]. Since the activation barrier for  $F_1$  is smaller than for  $F_2$ , and decreases with  $H$ , reversal of  $F_1$  due to such coupling explains the decrease of  $\tau_{AP}$  in the data of Fig. 2(c).

To summarize, we have demonstrated that simultaneous effects of ST on both magnetic layers in symmetric nanopillars determine their thermally activated behaviors. Our data indicate dynamical coupling between the magnetic layers mediated by ST, which may have a significant effect on the stability of magnetoelectronic devices and the efficiency of ST for magnetic reversal or excitation of dynamical states.

This work was supported by the NSF Grant DMR-0747609. NA and AH acknowledge support from the NASA Space Grant Consortium.

- 
- [1] J. Slonczewski, J. Magn. Magn. Mater. **159**, L1 (1996);  
 [2] L. Berger, Phys. Rev. **B 54**, 9353 (1996).  
 [3] J.A. Katine, F.J. Albert, R.A. Buhrman, E.B. Myers and D.C. Ralph, Phys. Rev. Lett. **84**, 3149 (2000).  
 [4] S. Urazhdin *et al.* (unpublished).  
 [5] M. Tsoi, J.Z. Sun, and S.S.P. Parkin, Phys. Rev. Lett. **93**, 036602 (2004).  
 [6] B. Ozyilmaz, A.D. Kent, M.J. Rooks, and J.Z. Sun, Phys. Rev. **B 71**, 140403 (2005).  
 [7] S. Urazhdin, H. Kurt, W.P. Pratt Jr., and J. Bass, Appl. Phys. Lett. **83**, 114 (2003).  
 [8] S.I. Kiselev, J.C. Sankey, I.N. Krivorotov, N.C. Emley, R.J. Schoelkopf, R.A. Buhrman, and D.C. Ralph, Nature **425**, 308 (2003).  
 [9] S. Urazhdin, N.O. Birge, W.P. Pratt Jr., and J. Bass, Phys. Rev. Lett. **91**, 146803 (2003).  
 [10] Z. Li and S. Zhang Phys. Rev. **B 69**, 134416 (2004).  
 [11] I.N. Krivorotov, N.C. Emley, A.G.F. Garcia, J.C. Sankey, S.I. Kiselev, D.C. Ralph, and R.A. Buhrman, Phys. Rev. Lett. **93**, 166603 (2004).